



Universiteit
Leiden
The Netherlands

Central role of semaphorin 3B in a serum-induced arthritis model and reduced levels in patients with rheumatoid arthritis

Igea, A.; Carvalheiro, T.; Malvar-Fernandez, B.; Martinez-Ramos, S.; Rafael-Vidal, C.; Niemantsverdriet, E.; ... ; Garcia, S.







Citation

Igea, A., Carvalheiro, T., Malvar-Fernandez, B., Martinez-Ramos, S., Rafael-Vidal, C., Niemantsverdriet, E., ... Garcia, S. (2022). Central role of semaphorin 3B in a serum-induced arthritis model and reduced levels in patients with rheumatoid arthritis. *Arthritis & Rheumatology*, 74(6), 972-983. doi:10.1002/art.42065

Version: Publisher's Version
License: [Creative Commons CC BY-NC 4.0 license](https://creativecommons.org/licenses/by-nc/4.0/)
Downloaded from: <https://hdl.handle.net/1887/3458791>

Note: To cite this publication please use the final published version (if applicable).

Central Role of Semaphorin 3B in a Serum-Induced Arthritis Model and Reduced Levels in Patients With Rheumatoid Arthritis

Ana Igea,¹ Tiago Carvalheiro,²  Beatriz Malvar-Fernández,³ Sara Martínez-Ramos,⁴ Carlos Rafael-Vidal,⁴ Ellis Niemantsverdriet,⁵  Jezabel Varadé,¹ Andrea Fernández-Carrera,¹ Norman Jimenez,⁴ Trudy McGarry,⁶ Angela Rodríguez-Trillo,⁷ Douglas Veale,⁸ Ursula Fearon,⁶  Carmen Conde,⁷ Jose M. Pego-Reigosa,⁴  África González-Fernández,¹  Kris A. Reedquist,² Timothy R. D. J. Radstake,² Annette van der Helm-Van Mil,⁵ and Samuel García³ 

Objective. Semaphorin 3B (Sema3B) decreases the migratory and invasive capacities of fibroblast-like synoviocytes (FLS) in rheumatoid arthritis (RA) and suppresses expression of matrix metalloproteinases. We undertook this study to examine the role of Sema3B in a mouse model of arthritis and its expression in RA patients.

Methods. Clinical responses, histologic features, and FLS function were examined in wild-type (WT) and Sema3B^{-/-} mice in a K/BxN serum transfer model of arthritis. Protein and messenger RNA expression of Sema3B in mouse joints and murine FLS, as well as in serum and synovial tissue from patients with arthralgia and patients with RA, was determined using enzyme-linked immunosorbent assay, immunoblotting, quantitative polymerase chain reaction, and RNA sequencing. FLS migration was determined using a wound closure assay.

Results. The clinical severity of serum-induced arthritis was significantly higher in Sema3B^{-/-} mice compared to WT mice. This was associated with increased expression of inflammatory mediators and increased migratory capacity of murine FLS. Administration of recombinant mouse Sema3B reduced the clinical severity of serum-induced arthritis and the expression of inflammatory mediators. Sema3B expression was significantly lower in the synovial tissue and serum of patients with established RA compared to patients with arthralgia. Serum Sema3B levels were elevated in patients with arthralgia that later progressed to RA, but not in those who did not develop RA; however, these levels drastically decreased 1 and 2 years after RA development.

Conclusion. Sema3B expression plays a protective role in a mouse model of arthritis. In RA patients, expression levels of Sema3B in the serum depend on the disease stage, suggesting different regulatory roles in disease onset and progression.

Dr. Carvalheiro's work was supported by the Portuguese National Funding Agency for Science, Research, and Technology (grants SFRH/BD/93526/2013 and SFRH/BD/116082/2016). Dr. Martínez-Ramos and Mr. Rafael-Vidal's work was supported by Xunta de Galicia (award IN606A-2021/024 to Dr. Martínez-Ramos and award IN606A-2020/043 to Mr. Rafael-Vidal). Dr. González-Fernández work was supported by the Xunta de Galicia Grupo Referencia Competitiva (grant ED431C 2016/041) and Centro de Investigaciones Biomédicas (co-financed by the European Regional Development Fund Operative Program ERDF Galicia 2014-2020 grant ERDF OP ED431G/02). Dr. García's work was supported by the Pfizer 2017 ASPIRE Dutch I CRP competitive grant program (grant WI229944), the Instituto de Salud Carlos III (project PI20/01472, co-funded by the European Regional Development Fund), and the Instituto de Salud Carlos III and European Social Fund Miguel Servet program (award CP19/00005).

¹Ana Igea, PhD, Jezabel Varadé, PhD, Andrea Fernández-Carrera, PhD, África González-Fernández, MD, PhD: Universidade de Vigo, Campus Universitario Lagoas Marcosende, and Galicia Sur Health Research Institute, Servicio Galego de Saúde Universidade de Vigo, Vigo, Spain; ²Tiago Carvalheiro, MSc, PhD, Kris A. Reedquist, PhD, Timothy R. D. J. Radstake, MD, PhD: University of Utrecht, Utrecht, The Netherlands; ³Beatriz Malvar-Fernández, BSc, Samuel García, PhD: University of Utrecht, Utrecht, The Netherlands, and Galicia Sur Health Research Institute and University

Hospital Complex of Vigo, Vigo, Spain; ⁴Sara Martínez-Ramos, DVM, Carlos Rafael-Vidal, MSc, Norman Jimenez, MSc, Jose M. Pego-Reigosa, MD, PhD: Galicia Sur Health Research Institute, Servicio Galego de Saúde Universidade de Vigo, and University Hospital Complex of Vigo, Vigo, Spain; ⁵Ellis Niemantsverdriet, PhD, Annette van der Helm-Van Mil, MD, PhD: Erasmus Medical Center, Rotterdam, The Netherlands, and Leiden University Medical Center, Leiden, the Netherlands; ⁶Trudy McGarry, PhD, Ursula Fearon, MD, PhD: St. Vincent's University Hospital and University College Dublin, and Trinity College Dublin, Dublin, Ireland; ⁷Angela Rodríguez-Trillo, PhD, Carmen Conde, MD, PhD: Hospital Clínico Universitario de Santiago de Compostela, Servicio Galego de Saúde, Santiago de Compostela, Spain; ⁸Douglas Veale, MD, PhD: St. Vincent's University Hospital and University College Dublin, Dublin, Ireland.

Author disclosures are available at <https://onlinelibrary.wiley.com/action/downloadSupplement?doi=10.1002%2Fart.42065&file=art42065-sup-0001-Disclosureform.pdf>.

Address correspondence to Samuel García, PhD, Rheumatology & Immune-mediated Diseases Iridis group, Galicia Sur Health Research Institute, Hospital Álvaro Cunqueiro, Estrada Clara Campoamor Number 341, 36312 Vigo, Pontevedra, Spain. Email: samuel.garcia@isgaliciasur.es.

Submitted for publication October 19, 2020; accepted in revised form January 4, 2022.

INTRODUCTION

Rheumatoid arthritis (RA) is an immune-mediated rheumatic and musculoskeletal disease marked by persistent synovial inflammation and progressive joint destruction, leading to disability and loss of quality of life (1,2). Most RA patients respond to the current therapies and reduction in disease progression is achieved; however, in 20–25% of patients, low disease activity is not reached. Moreover, current therapies have moderate-to-severe side effects, including higher cardiovascular risk and immunosuppression (3,4). Therefore, there is still an ultimate need for therapeutic molecules that can be targeted to reduce inflammation and joint destruction.

Semaphorin 3B (Sema3B) is a secreted protein belonging to the semaphorin family involved in different biologic processes, such as apoptosis, angiogenesis, cell migration, and invasion (5–7). A recent study from our group implicated Sema3B in the pathogenesis of RA (8). We have shown that Sema3B expression is reduced in the synovium of patients with early RA compared to patients with undifferentiated arthritis. Sema3B expression negatively correlated with clinical disease parameters and the expression of inflammatory mediators. Recombinant Sema3B reduces the migration and invasive capacity of RA fibroblast-like synoviocytes (FLS) in vitro (8). Taken together, these findings suggest that Sema3B might be a potential therapeutic target in RA. In the current study, we examined the functional role of Sema3B in a mouse model of arthritis and determined the local and systemic levels of Sema3B during the progression of RA.

PATIENTS AND METHODS

Patients and collection of samples. Serum samples and synovial biopsy specimens were obtained at the St. Vincent's University Hospital in Dublin, Ireland from patients with established RA who had clinically active inflamed joints ($n = 10$) and from patients with arthralgia ($n = 8$). Patients with arthralgia were defined as subjects with symptoms of aches and pains without clinical signs of synovitis or increased C-reactive protein levels (mean C-reactive protein level <5 mg/liter) but who were positive for circulating rheumatoid factor (RF+) and anti-citrullinated protein antibodies (ACPAs). Synovial biopsy specimens were obtained by needle arthroscopy from the knee joints, as previously described (9). Additionally, serum samples were obtained from the Leiden clinically suspect arthralgia (CSA) cohort (10) (Leiden University Medical Center, Leiden, The Netherlands), which is composed of 20 CSA patients with disease that progressed to RA, with paired samples at CSA onset and at the time that clinical arthritis first developed, and serum samples from 20 CSA patients with disease that did not progress to clinical arthritis or RA, in which paired samples were obtained at presentation of CSA and after 2 years of follow-up.

All patients presented at the outpatient clinic with recent-onset (<1 year) arthralgia of the small joints without clinical arthritis and had disease that, according to the clinical expertise of the rheumatologist, was suspected to progress to RA. Baseline visits consisted of physical examination, blood sample collection, and questionnaires. At the time of study inclusion, the autoantibody status of each patient was not known, as, in accordance with Dutch clinical practice guidelines, general practitioners are not required to measure serum autoantibodies as part of the examination. Follow-up visits were scheduled at months 4, 12, and 24. When necessary, additional visits were planned—for example, when a patient's symptoms increased or when a patient experienced joint swelling. Patients were followed up until the development of clinical inflammatory arthritis, determined by the rheumatologist at the time of the physical examination. During follow-up (and before the primary outcome was reached) treatment with disease-modifying antirheumatic drugs (including steroids) was not allowed. The date of censoring was either the date that the medical records were reviewed or an earlier date in those cases in which the patient was lost to follow-up.

In 8 CSA patients with disease that progressed to RA, serum samples were also obtained 1 year after diagnosis, and in 4 of these patients, serum samples were also obtained 2 years after diagnosis. All subjects provided written informed consent, and the protocol was approved by local institutional medical ethics review boards prior to patient inclusion in this study. RA patients fulfilled the American College of Rheumatology /European Alliance of Associations for Rheumatology 2010 classification criteria for RA (11,12). Clinical characteristics of the patients are detailed in Supplementary Tables 1–3 (available on the *Arthritis & Rheumatology* website at <http://onlinelibrary.wiley.com/doi/10.1002/art.42065/abstract>).

Serum-transfer arthritis and clinical scoring. K/BxN mouse serum was collected from 4–8-week-old arthritic K/BxN mice (provided by C. Benoist and D. Mathis [Harvard Medical School]). Arthritis was induced in wild-type (WT) and Sema3B^{-/-} mice (The Jackson Laboratory), transferring 100 μ l of K/BxN serum into 8–12-week-old mice by intraperitoneal (IP) injection on days 0 and 2. Alternatively, control phosphate buffered saline (PBS) vehicle, recombinant mouse Sema3B-Fc chimera protein, or mouse IgG2a isotype control (both 10 μ g) (R&D Systems) were administered IP on days 0, 2, and 4 in WT mice. Serum was collected on days 0, 4, and 9, and mice were killed on day 9 after serum transfer. Arthritis severity was assessed in each of the 4 limbs every 2 days by 2 blinded observers (AI and SG for evaluation of WT and Sema3B^{-/-} mice, and AR and CC for evaluation of recombinant Sema3B-treated mice) using a semiquantitative clinical score

*[Correction added on 12 May 2022, after first online publication: In Supplementary Table 1, the number (%) of patients with arthralgia receiving NSAIDs was changed from “0 (25)” to “2 (25).”]

(0 = no swelling, 1 = slight swelling and erythema of the ankle, wrist, or digits, 2 = moderate swelling and erythema, 3 = severe swelling and erythema, and 4 = maximal inflammation with joint rigidity for a maximum possible score of 16 points per mouse).

Histologic analysis. The hind limbs from mice killed on day 9 were prepared for histology by dissecting the skin and muscle and then sectioning the ankle joints. Specimens were fixed in formalin for 24 hours and were demineralized in Osteosoft (Merck Millipore) for 30 days. Ankle joints were embedded in paraffin, cut, and stained with hematoxylin and eosin to evaluate inflammation and bone erosion. Toluidine blue was used for analysis of cartilage damage.

Synovial inflammation was graded according to the following index, where 0 = no inflammation, 1 = slight thickening of the synovial cell layer and/or some inflammatory cells in the sublining, 2 = thickening of the synovial lining and moderate infiltration of the sublining, 3 = thickening of the synovial lining and marked infiltration, and 4 = thickening of the synovial lining and severe infiltration. Cartilage damage was evaluated using a 0–4–point scale, where 0 = normal cartilage, 1 = cartilage surface irregularities and loss of metachromasia adjacent to superficial chondrocytes, 2 = fibrillation of cartilage with minor loss of surface cartilage, 3 = moderate cartilage abnormalities, including loss of superficial cartilage and moderate multifocal chondrocyte loss, and 4 = marked cartilage destruction with extension of fissures close to subchondral bone. Bone erosions were scored on a 0–4–point scale, where 0 = normal bone, 1 = small resorption areas, 2 = more numerous resorption areas, 3 = obvious resorption, and 4 = full-thickness resorption areas in the bone.

Mouse FLS culture and stimulation. Mouse FLS were isolated from WT and *Sema3B*^{-/-} mice. Synovial tissue was minced and incubated with 1 mg/ml of collagenase in serum-free Dulbecco's modified Eagle's medium (DMEM) (Invitrogen) at 37°C for 3 hours. After digestion, FLS were passed through a nylon cell strainer (BD Falcon), washed, and cultured in 10% fetal bovine serum (FBS) (BioWest) and 10,000 units/ml of penicillin/streptomycin (ThermoFisher Scientific). After culture overnight, nonadherent cells were removed, and adherent cells were cultured in DMEM–10% FBS and used between passages 4 and 6.

Sema3B and cytokine measurement. *Sema3B* (Biomatik) levels in the serum of patients with arthralgia and patients with RA, *Sema3B* (Abbexa) levels in the serum of arthritic mice, and interleukin-6 (IL-6) (eBioscience) and tumor necrosis factor (TNF) (R&D Systems) levels in cell-free assay supernatants of mouse FLS were measured using an enzyme-linked immunosorbent assay, according to the manufacturer's instructions.

Bulk messenger RNA (mRNA) sequencing protocol. Sequencing was performed by the sequencing service provider

Single Cell Discoveries, using an adapted version of the CEL-Seq protocol. Total RNA from mouse forepaws was extracted using an RNeasy kit and an RNase-Free DNase set (Qiagen) and was used for library preparation and sequencing. We processed mRNA as described previously, following an adapted version of the single-cell mRNA sequencing protocol of CEL-Seq (13,14). In brief, samples were barcoded with CEL-Seq primers during reverse transcription and were pooled after second-strand synthesis. The resulting complementary DNA (cDNA) was amplified with an overnight in vitro transcription reaction. From this amplified RNA, sequencing libraries were prepared with Illumina TruSeq small RNA primers.

Paired-end sequencing was performed on the Illumina NextSeq 500 platform. Read 1 was used to identify the Illumina library index and CEL-Seq sample barcode. Read 2 was aligned to the *Mus musculus* GRCm38 (mm10) mouse reference transcriptome using BWA (15). Reads that mapped equally well to multiple locations were discarded. Mapping and generation of count tables was conducted using the MapAndGo script (<https://github.com/anna-alemany/transcriptomics/tree/master/mapandgo>). Samples were normalized using reads per million-mapped reads normalization. The differential expression analysis based on the negative binomial was performed using R/Bioconductor package DESeq2 version 1.32. Negative binomial generalized linear model fitting and a paired Wald's test was used to assess the differentially expressed genes (DEGs), and *P* values were adjusted for multiple testing errors with a 5% false discovery rate according to the Benjamini-Hochberg method (16). DEGs were defined as those genes showing a ≥ 2 fold change in expression at an adjusted *P* value (*P*_{adj}) less than 0.05.

Real-time polymerase chain reaction (PCR) and quantitative PCR (qPCR). RNA from mouse forepaws, mouse FLS, and synovial tissue was isolated using an RNeasy Kit and an RNase-Free DNase Set (Qiagen). Total RNA was reverse-transcribed using iScript (Bio-Rad). Duplicate PCRs were performed using SYBR Green (Applied Biosystems) with a StepOnePlus Real-Time PCR detection system (Applied Biosystems). We amplified cDNA using specific primers (all from IDT) (see Supplementary Tables 4 and 5, <http://onlinelibrary.wiley.com/doi/10.1002/art.42065/abstract>). Relative levels of gene expression were normalized to the expression levels of 3 housekeeping genes (*B2M*, *RPL13*, and *RPL32* or *Hprt*, β -actin, and *B2m*). Relative expression was calculated using the formula $2^{-\Delta\Delta C_t} \times 1,000$.

Immunoblotting. FLS were lysed in Laemmli buffer and forepaws were lysed in radioimmunoprecipitation assay buffer. Protein content was quantified with a BCA Protein Assay kit (Pierce). An equal amount of total protein was subjected to electrophoresis on 4–12% NuPAGE Bis-Tris gels (Invitrogen), and

proteins were transferred to PVDF membranes (Millipore). Membranes were incubated overnight at 4°C with the following primary antibodies: antibodies specific to TNF (BD PharMingen); Sema3B, ERK, and β -actin antibodies (all from Abcam); neuropilin 1, plexin A2, and tubulin antibodies (all from R&D Systems); and H3 and protein ERK antibodies (Santa Cruz Biotechnology). Membranes were then washed and incubated in Tris buffered saline–Tween containing a horseradish peroxidase–conjugated secondary antibody. Protein was detected with Lumi-Light Plus Western blotting substrate (Roche Diagnostics) using a Chemi-Doc MP imaging system (Bio-Rad). Densitometry analysis was performed with ImageJ software. Relative protein expression was normalized to the values for H3, tubulin, or β -actin.

Migration assay. Cell migration was determined using a wound closure motility assay. A linear scratch was made on

cultured mouse FLS plated at confluence using a 200- μ l micropipette tip and then washed with PBS to remove unattached cells. Mouse FLS were placed in medium containing 1% or 10% FBS, and thereafter were either left unstimulated or stimulated with recombinant mouse Sema3B (100 ng/ml) (R&D Systems). Light microscopy images were obtained immediately (time point 0) and 24 hours after wounding. The mean number of migrated cells was determined from 3 10 \times field-of-view images and values were normalized to those in cultures with unstimulated cells.

Statistical analysis. A statistical analysis was performed using Windows GraphPad Prism version 8. Potential differences between patient groups were analyzed using a nonparametric 2-tailed Mann-Whitney test or a Kruskal-Wallis test, as appropriate. Potential differences between the mouse groups were

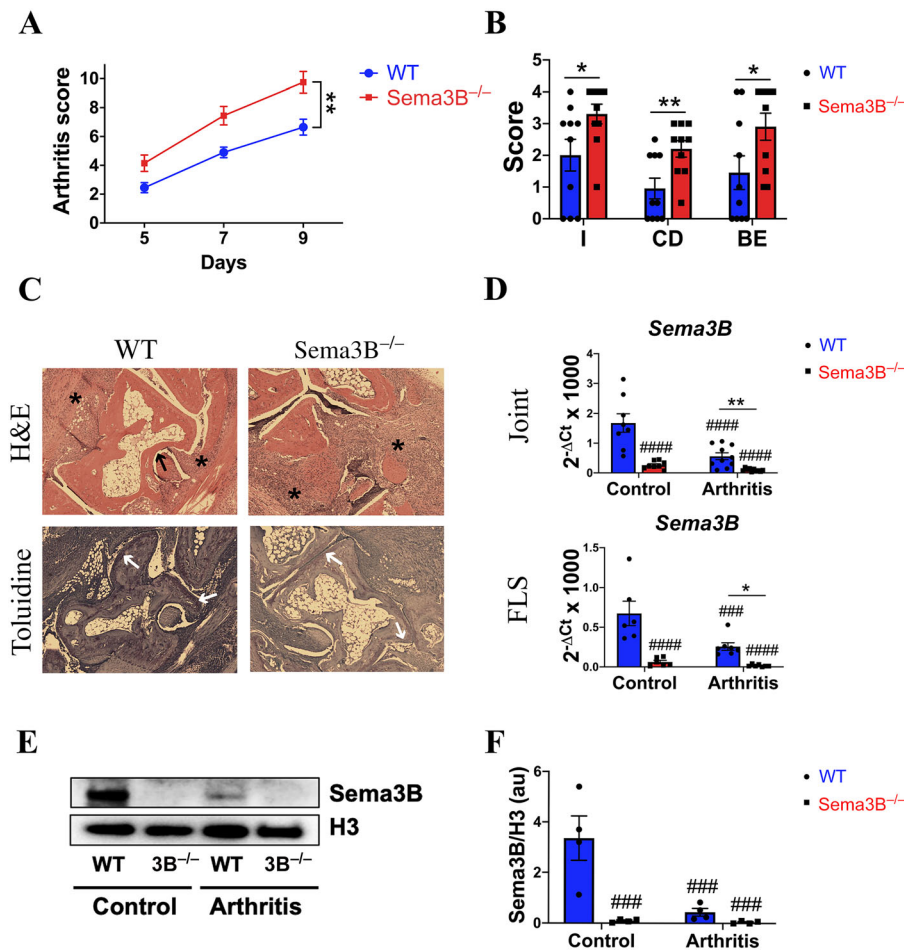


Figure 1. Semaphorin 3B (Sema3B) deficiency increases the severity of serum-induced arthritis. **A**, Daily global arthritis scores in wild-type (WT) mice ($n = 10$) and Sema3B^{-/-} mice ($n = 10$). Values are the mean \pm SEM. **B**, Inflammation (I) scores, cartilage damage (CD) scores, and bone erosion (BE) scores in mice in each group. **C**, Representative images of histologic features in the mouse joints, visualized using hematoxylin and eosin (H&E) and toluidine blue staining ($n = 10$). Synovial cell infiltration (asterisks), bone erosion (black arrow), and cartilage damage (white arrows) are shown. **D**, Expression of Sema3B mRNA in the joints and fibroblast-like synoviocytes (FLS) of WT mice ($n = 6-8$) and Sema3B^{-/-} mice ($n = 6-8$). **E** and **F**, Representative immunoblot (**E**) and densitometric analysis (**F**) of Sema3B expression in FLS from WT mice ($n = 4$) and Sema3B^{-/-} mice ($n = 4$). In **B**, **D**, and **F**, symbols represent individual mice; bars show the mean \pm SEM. * = $P < 0.05$; ** = $P < 0.01$. ### = $P < 0.001$; #### = $P < 0.0001$, versus nonarthritic WT control mice.

analyzed using a parametric Student's 2-tailed paired *t*-test or analysis of variance, as appropriate. *P* values less than 0.05 were considered statistically significant.

RESULTS

Higher severity of arthritis in *Sema3B*^{-/-} mice. We initially analyzed the role of *Sema3B* in K/BxN serum-induced arthritis and found that the clinical severity of arthritis was significantly higher in *Sema3B*^{-/-} mice compared to the WT mice (Figure 1A). These differences were not sex dependent (Supplementary Figure 1A, <http://onlinelibrary.wiley.com/doi/10.1002/art.42065/>

abstract). Histologic analysis of the tibiotar and forefoot joints revealed significant increases in synovial inflammation, cartilage damage, and bone erosion in the *Sema3B*^{-/-} mice (Figures 1B and C and Supplementary Figure 1B).

Next, we determined the expression of *Sema3B* in the total joints and FLS of mice. As expected, expression of *Sema3B* mRNA and protein was not detected in either the nonarthritic control group or the arthritic group of *Sema3B*^{-/-} mice. Remarkably, among WT mice, expression of *Sema3B* was significantly lower in the arthritic group compared to the nonarthritic group (Figures 1D–F). Taken together, these data suggest that *Sema3B* may play a protective role in the K/BxN serum-induced arthritis model.

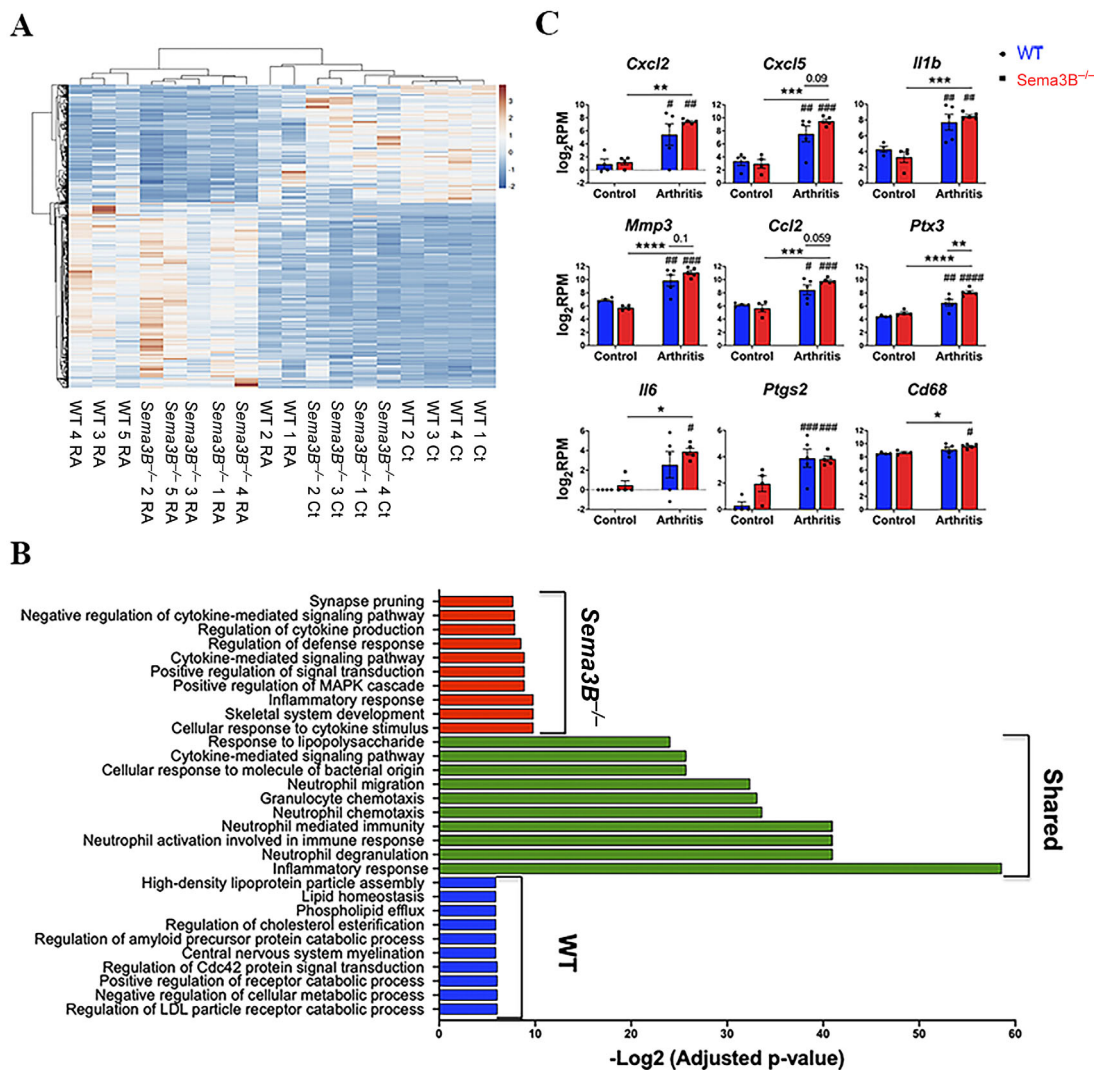


Figure 2. *Sema3B* deficiency enhances the activation of inflammatory pathways. **A**, Expression of differentially expressed gene (DEG) mRNA in the forepaws of WT or *Sema3B*^{-/-} mice in a model of rheumatoid arthritis (RA) (*n* = 5 each) relative to that in nonarthritic control (Ct) mice (*n* = 4). Data are presented as a heatmap showing the lowest (blue) and highest (orange) mRNA expression levels. **B**, Gene Ontology analysis of the biologic processes associated with DEGs specific to arthritic WT mice, those specific to arthritic *Sema3B*^{-/-} mice, or those shared between both groups. **C**, Expression of mRNA for inflammatory mediators, analyzed by RNA-Seq in the forepaws of nonarthritic control mice (*n* = 4) and arthritic WT mice or *Sema3B*^{-/-} mice (*n* = 5). Symbols represent individual mice; bars show the mean ± SEM. * = *P* < 0.05; ** = *P* < 0.01; *** = *P* < 0.001; **** = *P* < 0.0001. # = *P* < 0.05; ## = *P* < 0.01; ### = *P* < 0.001; #### = *P* < 0.0001, versus nonarthritic WT control mice. LDL = low-density lipoprotein (see Figure 1 for other definitions). Color figure can be viewed in the online issue, which is available at <http://onlinelibrary.wiley.com/doi/10.1002/art.42065/abstract>.

Enhanced activation of inflammatory pathways in *Sema3B*^{-/-} mice. To explore the mechanisms underlying increased arthritis severity in *Sema3B*^{-/-} mice, we performed an RNA sequencing analysis in the joints of control mice and arthritic mice. A principal components analysis of the whole transcriptome showed a clearer distinction between the control and arthritic groups rather than between WT mice and *Sema3B*^{-/-} mice (Supplementary Figure 2A, <http://onlinelibrary.wiley.com/doi/10.1002/art.42065/abstract>). In fact, there were no significant differences between WT and *Sema3B*^{-/-} nonarthritic control mice, and we only observed a trend toward down-regulated expression of *Sema3B* mRNA in *Sema3B*^{-/-} mice (fold change 0.06; $P_{\text{adj}} = 0.078$) (data not shown).

Next, we compared gene expression levels between WT and *Sema3B*^{-/-} arthritic mice and, similar to the control groups, we did not observe major differences. In fact, only 2 genes (*Sema3b* and *Lrrm4cl*) were found to have significantly lower expression in *Sema3B*^{-/-} mice compared to WT mice (Supplementary Table 6, <http://onlinelibrary.wiley.com/doi/10.1002/art.42065/abstract>).

We therefore compared the DEGs in WT or *Sema3B*^{-/-} arthritic mice relative to WT control mice. The results revealed 197 DEGs in arthritic WT mice and 566 DEGs in arthritic *Sema3B*^{-/-} mice that showed significant differences in expression compared to nonarthritic controls (Supplementary Tables 7 and 8, <http://onlinelibrary.wiley.com/doi/10.1002/art.42065/abstract>). A heatmap of the DEGs clearly distinguished the nonarthritic control mice and arthritic mice. Importantly, the *Sema3B*^{-/-} arthritic mice clustered together, while the WT arthritic mice grouped in 2 different clusters, with 1 more similar to the *Sema3B*^{-/-} arthritic mice and the other more similar to the nonarthritic mice (Figure 2A). Subsequently, we performed a venn diagram analysis (17) and we found that of all DEGs (606), 40 (6.6%) were specific to WT mice, 409 (67.5%) were specific to *Sema3B*^{-/-} mice, and 157 (25.9%) were differentially expressed in both groups (Supplementary Figure 2B and Supplementary Table 9, <http://onlinelibrary.wiley.com/doi/10.1002/art.42065/abstract>). A Gene Ontology analysis of biologic processes did not show any relevant pathways in those DEGs

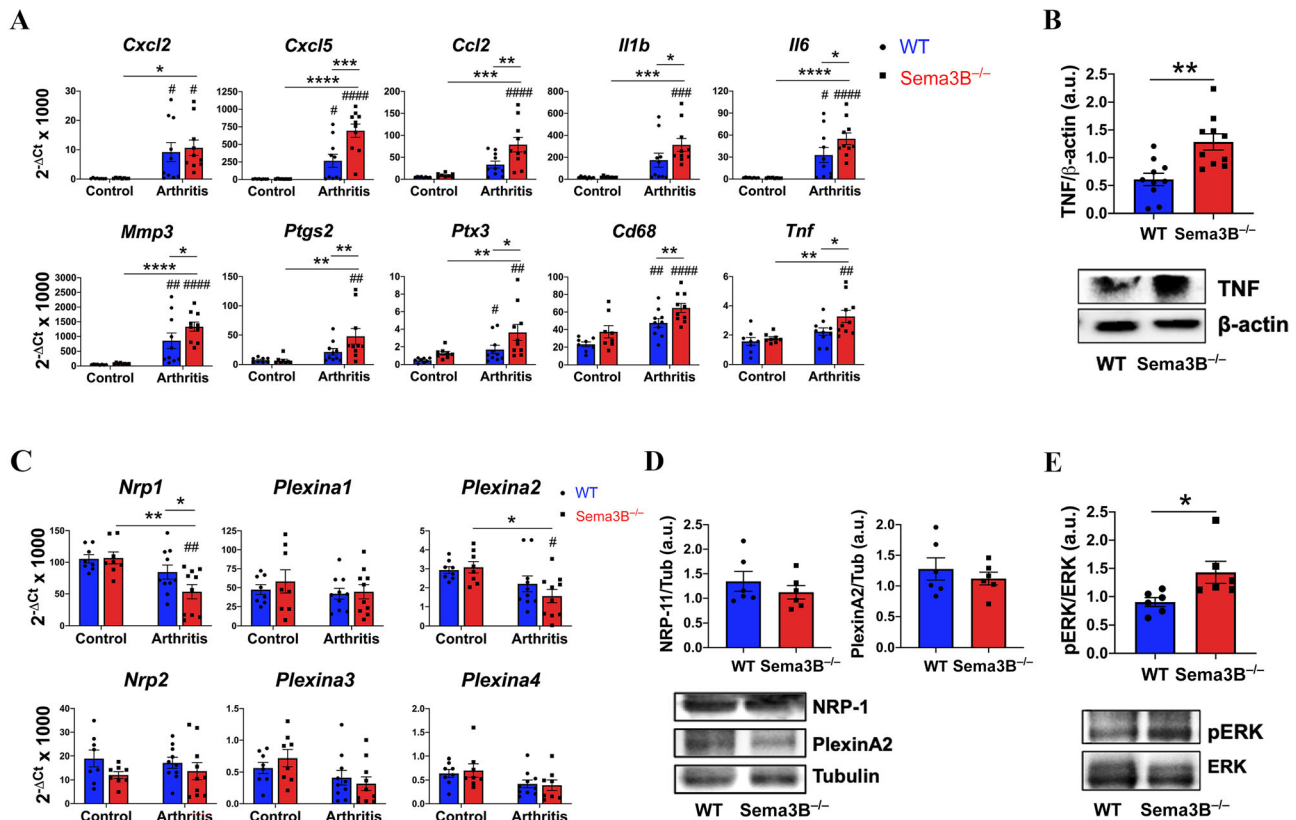


Figure 3. *Sema3B* deficiency enhances the activation of inflammatory pathways. **A**, Expression of mRNA for inflammatory mediators analyzed by quantitative PCR (qPCR) of the forepaws in nonarthritic control mice ($n = 8$) and arthritic WT mice or *Sema3B*^{-/-} mice ($n = 10$). **B**, Densitometric analysis and representative immunoblot of tumor necrosis factor (TNF) in the joints of arthritic WT mice ($n = 10$) and arthritic *Sema3B*^{-/-} mice ($n = 10$). **C**, Expression of *Sema3B* mRNA receptors analyzed by qPCR of the forepaws of nonarthritic control mice ($n = 8$) and arthritic WT mice or *Sema3B*^{-/-} mice ($n = 10$ each). **D** and **E**, Densitometric analysis and representative immunoblot of neuropilin 1 (NRP-1) and plexin A2 expression (**D**) and ERK activation (**E**) in the joints of arthritic WT mice ($n = 6$) and arthritic *Sema3B*^{-/-} mice ($n = 6$). Symbols represent individual mice; bars show the mean \pm SEM. * = $P < 0.05$; ** = $P < 0.01$; *** = $P < 0.001$; **** = $P < 0.0001$. # = $P < 0.05$; ## = $P < 0.01$; ### = $P < 0.001$; #### = $P < 0.0001$, versus nonarthritic WT control mice. Tub = tubulin (see Figure 1 for other definitions). Color figure can be viewed in the online issue, which is available at <http://onlinelibrary.wiley.com/doi/10.1002/art.42065/abstract>.

specific to the WT arthritic group. As expected, the DEGs shared between both groups are related to processes involved in the pathogenesis of arthritis in this murine model, such as inflammatory responses, neutrophil activation and migration, and cytokine-mediated signaling pathways. In addition, the biologic processes specific to the *Sema3B*^{-/-} mice were also related to cytokine and inflammatory responses (Figure 2B and Supplementary Table 10, <http://onlinelibrary.wiley.com/doi/10.1002/art.42065/abstract>).

We analyzed several DEGs common to WT and *Sema3B*^{-/-} arthritic mice (*Cxcl2*, *Cxcl5*, *Il1b*, *Ccl2*, *Mmp3*, and *Ptx3*) and some specific to arthritic *Sema3B*^{-/-} mice (*Il6*, *Ptgs2*, and *Cd68*), and we found elevated expression in the arthritic *Sema3B*^{-/-} mice compared to arthritic WT mice, although only the difference in *Ptx3* expression was significant (Figure 2C). In

order to confirm these data, we analyzed this subset of genes using single qPCR, as well as *Tnf*, due to the key role it plays in RA pathogenesis (2,18). We found up-regulation of *Cxcl5*, *Ccl2*, *Tnf*, *Il1*, *Il6*, *Mmp3*, *Ptgs2*, *Cd68*, and *Ptx3* in arthritic WT mice and arthritic *Sema3B*^{-/-} mice compared to the nonarthritic control mice and significantly enhanced expression in arthritic *Sema3B*^{-/-} mice compared to arthritic WT mice (Figure 3A). Finally, we also validated the increased expression of TNF at the protein level (Figure 3B).

Next, we investigated the possible molecular mechanisms involved in the elevated severity of arthritis in this murine model. First, we analyzed expression of the *Sema3B* receptors, the plexin A family members, and the coreceptors neuropilin 1 (NRP-1) and NRP-2 (5–7,19). We found that expression of *Nrp1* and *Plexina2* was significantly lower in the joints of arthritic

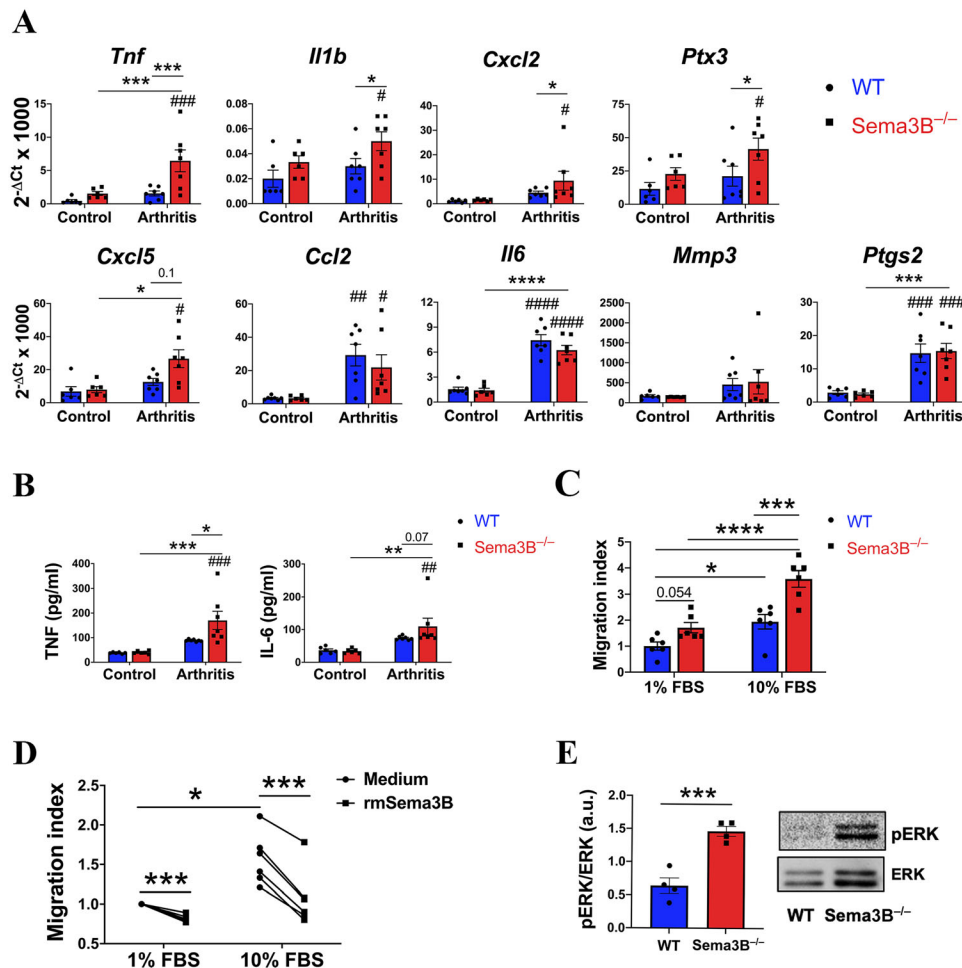


Figure 4. *Sema3B* deficiency enhances activation of inflammatory pathways and the migratory capacity of FLS. **A** and **B**, Expression of mRNA for inflammatory mediators (**A**) and tumor necrosis factor (TNF) and interleukin-6 (IL-6) protein secretion (**B**) in FLS (at passage 4) from nonarthritic control mice ($n = 6$) and arthritic WT mice or *Sema3B*^{-/-} mice ($n = 7$). **C**, Migration of FLS (at passage 4) from arthritic WT mice and arthritic *Sema3B*^{-/-} mice after culture in 1% or 10% fetal bovine serum (FBS) for 24 hours. **D**, Migration of mouse FLS (at passage 6) from arthritic *Sema3B*^{-/-} mice stimulated with recombinant mouse *Sema3B* (rmSema3B) (100 ng/ml) after culture in 1% or 10% FBS for 24 hours. **E**, Densitometric analysis and representative immunoblot of ERK activation in FLS (at passage 4) from arthritic WT mice ($n = 4$) and arthritic *Sema3B*^{-/-} mice ($n = 4$). In **A–C** and **E**, symbols represent individual mice; bars show the mean \pm SEM. * = $P < 0.05$; ** = $P < 0.01$; *** = $P < 0.001$; **** = $P < 0.0001$. # = $P < 0.05$; ## = $P < 0.01$; ### = $P < 0.001$; ##### = $P < 0.0001$, versus nonarthritic WT control mice. See Figure 1 for other definitions. Color figure can be viewed in the online issue, which is available at <http://onlinelibrary.wiley.com/doi/10.1002/art.42065/abstract>.

Sema3B^{-/-} mice compared to the joints of WT and Sema3B^{-/-} nonarthritic mice. In addition, expression of *Nrp1* was also diminished compared to levels in arthritic WT mice (Figure 3C). At the protein level, we observed slightly reduced expression of NRP-1 and plexin A2 in arthritic Sema3B^{-/-} mice compared to arthritic WT mice, although this difference was not statistically significant (Figure 3D).

As Sema3B reduces ERK activation in FLS (8), we also evaluated the activation of this protein kinase in mouse FLS. In addition, 1 of the pathways found in the RNA-Seq data specific to arthritic Sema3B^{-/-} mice was the positive regulation of the MAPK cascade (Figure 2B). Consistent with this finding, our results showed significantly increased ERK activation in arthritic Sema3B^{-/-} mice compared to arthritic WT mice (Figure 3E).

Enhanced inflammatory and migratory phenotype of FLS in Sema3B^{-/-} mice. In arthritic mouse FLS, we further analyzed expression of the gene targets in the joint tissue, since Sema3B is mainly expressed by FLS in the synovium (8). Our qPCR analysis showed increased *Tnf*, *Il1*, *Ptx3*, *Cxcl2*, and *Cxcl5* expression in FLS from arthritic Sema3B^{-/-} mice compared to FLS from arthritic WT mice, but there were no differences in terms of the expression of *Ccl2*, *Il6*, *Mmp3*, or *Ptgs2* (Figure 4A). At the

protein level, secretion of TNF and IL-6 was also increased in FLS from arthritic Sema3B^{-/-} mice (Figure 4B).

Since Sema3B impairs the migratory capacity of RA FLS (8), we analyzed the migratory capacity of mouse FLS. We observed a trend toward increased spontaneous migration and significantly higher FBS-induced migration in FLS from Sema3B^{-/-} mice compared to FLS from arthritic WT mice. Notably, the higher degree of migration of FLS from Sema3B^{-/-} mice was reverted after stimulation with recombinant mouse Sema3B (Figures 4C and D).

Lastly, we determined ERK activation and, similar to the observations in the total joints of mice, ERK activation was significantly increased in the FLS from arthritic Sema3B^{-/-} mice compared to WT mice (Figure 4E).

Protective role of Sema3B in a murine model of arthritis. To confirm that Sema3B plays a protective role in this model of arthritis, we determined the effect of treatment with a recombinant mouse Sema3B fusion protein in arthritic WT mice. Arthritis severity was significantly lower in recombinant mouse Sema3B-treated mice compared to mice in both control groups (PBS and isotype control IgG) (Figure 5A). Consistent with this, histologic analysis at day 9 showed a drastic reduction in synovial

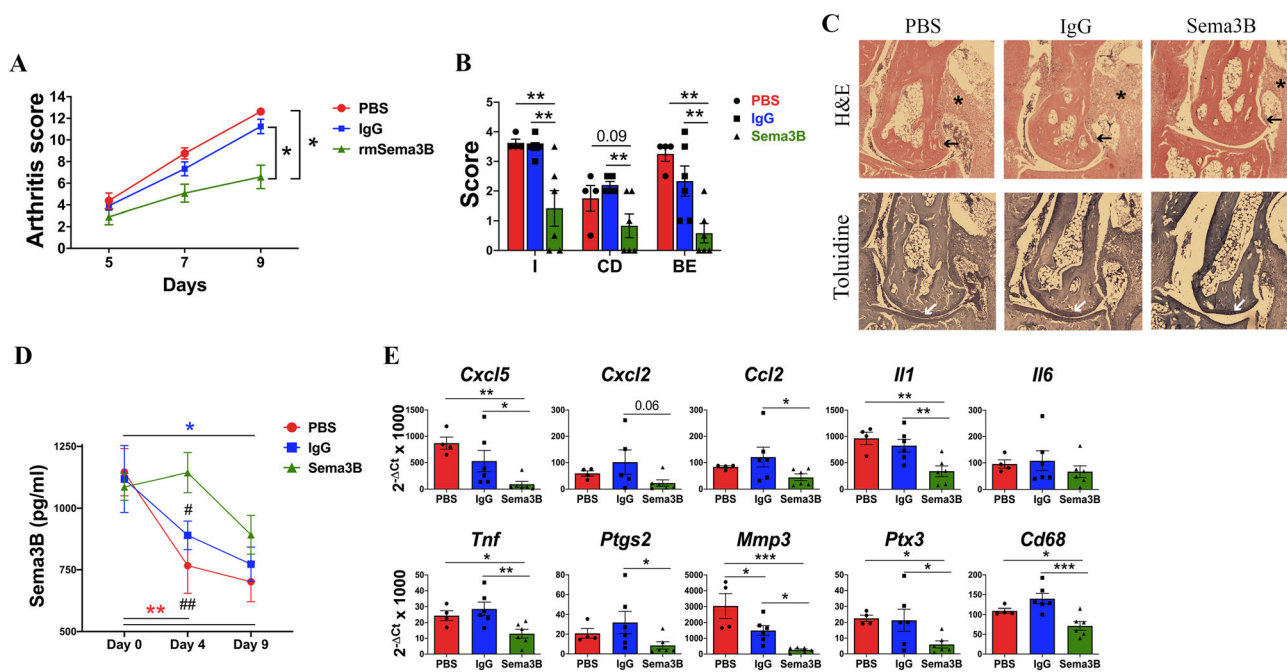


Figure 5. Sema3B reduces the severity of serum-induced arthritis. **A**, Daily global arthritis scores in arthritic WT mice treated on days 0, 2, and 4 with control phosphate buffered saline (PBS) ($n = 4$), isotype control IgG ($10 \mu\text{g}$) ($n = 6$), or recombinant mouse Sema3B (rmSema3B) ($10 \mu\text{g}$) ($n = 6$). Values are the mean \pm SEM. **B**, Inflammation scores, cartilage damage scores, and bone erosion scores in mice in each group. **C**, Representative images of histologic features in the mouse joints visualized with H&E and toluidine blue staining. Synovial cell infiltration (asterisks), bone erosion (black arrows), and cartilage damage (white arrows) are shown. **D**, Longitudinal serum Sema3B levels in the mouse groups analyzed in **A**. **E**, Expression of mRNA for inflammatory mediators in the forepaws of mice analyzed in **A**. In **B** and **E**, symbols represent individual mice; bars show the mean \pm SEM. * = $P < 0.05$; ** = $P < 0.01$; *** = $P < 0.001$. # = $P < 0.05$; ## = $P < 0.01$, versus Sema3B-treated mice on day 4. See Figure 1 for other definitions. Color figure can be viewed in the online issue, which is available at <http://onlinelibrary.wiley.com/doi/10.1002/art.42065/abstract>.

inflammation, cartilage damage, and bone erosion in recombinant mouse *Sema3B*-treated mice compared to those in both control groups (Figures 5B and C).

Findings from a longitudinal analysis demonstrated that serum *Sema3B* levels were significantly lower during the course of arthritis in the PBS and IgG groups. In the *Sema3B*-treated group, the levels of this protein on day 4 were similar to those observed on day 0 (before the induction of arthritis and administration of the recombinant mouse *Sema3B*), but were reduced on day 9, likely due to the final dose of recombinant mouse *Sema3B* administered on day 4. Importantly, also on day 4, levels of *Sema3B* were significantly higher in the *Sema3B* mouse group compared to the control groups (Figure 5D). Finally, analysis of the inflammatory mediators in the mouse joints demonstrated that recombinant mouse *Sema3B* administration resulted in significantly down-regulated expression of *Tnf*, *Il1*, *Ccl2*, *Cxcl5*, *Ptgs2*, *Ptx3*, *Cd68*, and *Mmp3* compared to the expression levels of these genes in the control groups (Figure 5E).

Disease stage dependence of *Sema3B* expression in human RA. Our previous findings (8) and results from the murine experiments suggest that *Sema3B* expression might be reduced in patients with established RA, but to date its expression in patients with arthralgia preceding the development of clinical arthritis and RA is unexplored. First, we examined the local and

systemic expression of *Sema3B* in patients with arthralgia and those with RA. We found significantly lower *Sema3B* mRNA and protein expression in the synovial tissue and serum of patients with established RA compared to those with arthralgia (Figures 6A and B).

To better understand the expression levels at different disease stages, we measured *Sema3B* levels in 20 patients with CSA who had disease that progressed to RA (median time between presentation with CSA and the development of clinical arthritis 4 months [interquartile range 0.3–5]) and 20 patients with disease that did not progress to RA (samples collected at presentation with CSA and after 2 years). In patients with disease that progressed to RA, serum *Sema3B* levels were significantly elevated both at the time of presentation with CSA and at the time that clinical arthritis first developed, compared to the levels in the patients who had disease that did not progress to RA (Figure 6C).

These differences were independent of ACPA autoantibody status, as *Sema3B* levels were increased in the progressor patients in both the ACPA-negative and ACPA-positive groups. Interestingly, at the baseline visit and to a lower extent after 1 year of follow-up, levels of *Sema3B* were significantly higher in ACPA-positive patients compared to ACPA-negative patients, both in those with disease that progressed to RA and in those whose disease remained as arthralgia (Supplementary Figure 3 <http://onlinelibrary.wiley.com/doi/10.1002/art.42065/abstract>). Similar

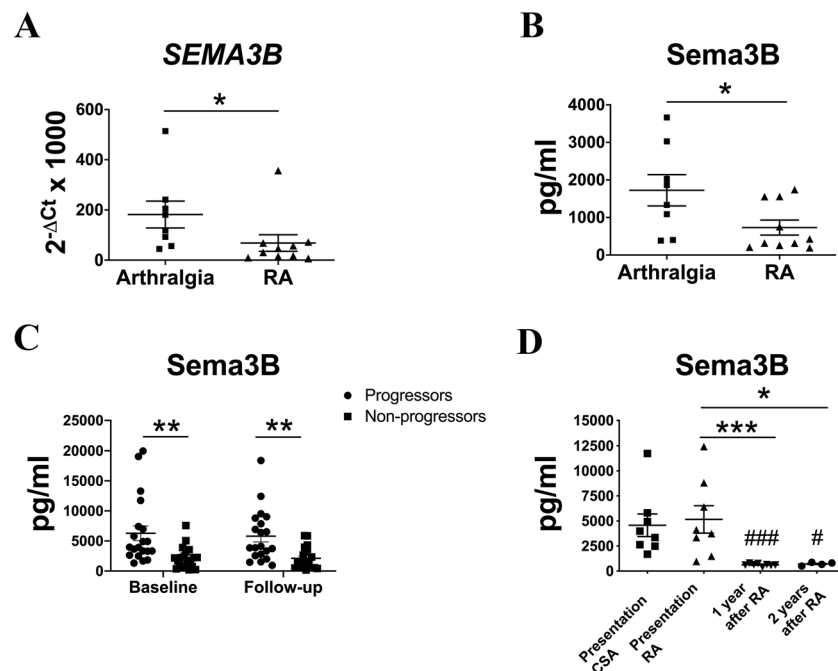


Figure 6. Semaphorin 3B (*Sema3B*) expression is reduced during the progression of rheumatoid arthritis (RA). **A** and **B**, Expression of *Sema3B* mRNA in synovial tissue (**A**) and *Sema3B* protein in serum (**B**) from patients with arthralgia ($n = 8$) and those with established RA ($n = 10$). **C**, *Sema3B* levels in a longitudinal cohort of patients with clinically suspect arthralgia (CSA) ($n = 40$) who had disease that progressed to RA ($n = 20$) or those whose disease remained as arthralgia after 2 years of follow-up ($n = 20$). **D**, *Sema3B* levels in a longitudinal cohort of patients with CSA at presentation of arthralgia ($n = 8$), at presentation of RA ($n = 8$), and 1 year ($n = 8$) and 2 years ($n = 4$) after RA diagnosis. Symbols represent individual patients; bars show the mean \pm SEM. * = $P < 0.05$; ** = $P < 0.01$; *** = $P < 0.001$. # = $P < 0.05$, ### = $P < 0.001$, versus presentation.

to the previous set of patients with established RA, in 8 of the CSA patients with disease that progressed to RA, *Sema3B* levels were drastically reduced after 1 year of follow-up, and in 4 patients, levels remained lower after 2 years of follow-up (Figure 4D). Taken together, these data show that expression of *Sema3B* is disease stage-dependent and is associated with ACPA status.

DISCUSSION

In this study we found that *Sema3B* plays a protective role in a K/BxN mouse model of arthritis. The higher arthritis severity observed in *Sema3B*^{-/-} mice was associated with 2 main effects. First, mRNA and protein analysis in *Sema3B*^{-/-} mice showed higher expression of cytokines, chemokines, and matrix metalloproteinases, which are elevated in RA patients and play a key role in pathogenesis of the disease (18,20,21). Enrichment analysis of DEGs in both WT arthritic mice and *Sema3B*^{-/-} arthritic mice showed induction of biologic pathways involved in the pathogenesis of arthritis in this model, as well as in RA patients. Specific pathways in *Sema3B*^{-/-} mice were also related to these processes, indicating that *Sema3B* deficiency enhances the expression of inflammatory mediators, rather than regulating other biologic processes. We found that FLS are responsible for the enhanced expression of inflammatory mediators, although some mediators were up-regulated in total joints but not in FLS (*Il6*, *Ccl2*, *Mmp3*, *Ptgs2*), suggesting the involvement of other cell types. Neutrophils and macrophages are crucial in a K/BxN mouse model of arthritis, as they represent the main immune cells infiltrating the affected joints and release cytokines and chemokines, among other inflammatory mediators (22–24).

Increased synovial inflammation and higher expression of the macrophage marker CD68 in the joints of *Sema3B*^{-/-} mice suggest that both neutrophils and macrophages are involved in the greater arthritis severity and in the production of inflammatory mediators found in these mice. Second, FLS from *Sema3B*^{-/-} mice demonstrated an increased migratory capacity, consistent with the invasive and aggressive phenotype of RA FLS (8,25,26). In addition, the enhanced bone erosion observed in *Sema3B*^{-/-} mice suggests that *Sema3B* also may be involved in bone erosion, which is consistent with findings from other studies that have shown that *Sema3B* promotes osteoblastic proliferation and differentiation (27,28).

In this study we also found lower expression of plexin A2 and the coreceptor NRP-1 in the joints of WT arthritic mice, and this reduction was more evident in the *Sema3B*^{-/-} arthritic mice. These data, taken together with the low *Sema3B* levels, suggest that decreased plexin A2 and NRP-1 expression may be implicated in this arthritis model. In fact, plexin A2 and NRP-1 are crucial for appropriate *Sema3B* signaling in different cell types (8,29,30). In addition, *Sema3A* and *Sema3F*, which play protective roles in RA pathogenesis, also bind to plexin A2 and NRP-1. Therefore, *Sema3B* deficiency might also enhance arthritis

severity through the impairment of the *Sema3A* and *Sema3F* protective pathways. (8,31,32).

Regarding the molecular pathways involved in enhanced arthritis severity, we found higher ERK activation both in the joints and in the FLS from *Sema3B*^{-/-} arthritic mice, indicating that the protective role of *Sema3B* in RA pathogenesis may be due, at least in part, to inhibition of this molecular pathway. This notion is supported by previous findings of low ERK activation in *Sema3B*-stimulated RA FLS (8) and elevated ERK activation in synovial tissue from patients with RA, as well as from patients with early arthritis who develop erosive RA (33–35).

Notably, expression of *Sema3B* was reduced in arthritic WT mice during the course of arthritis, similar to the decreased *Sema3B* levels observed during RA progression. Of special interest, administration of *Sema3B* resulted in diminished arthritis severity, decreased expression of inflammatory mediators, and reduced migration of FLS, highlighting the important modulatory role of *Sema3B* in the K/BxN mouse model of arthritis.

We also found that local and systemic levels of *Sema3B* were lower in patients with established RA compared to patients with arthralgia; however, *Sema3B* levels were increased in patients with CSA who had disease that progressed to RA. These data suggest that expression of *Sema3B* is disease stage dependent and the elevated expression in patients with pre-RA may be a consequence of a counterregulatory mechanism, similar to the high levels of antiinflammatory mediators (IL-4, IL-5, IL-10, IL-13) observed in patients with RA (35–37). Due to the protective role of *Sema3B*, this counterregulation in the early stages of the disease may reduce the pathogenic processes that ultimately lead to joint destruction. However, further studies are needed to elucidate this mechanism. Eight of the CSA patients with disease that progressed to RA presented with remarkably low serum *Sema3B* levels 1 and 2 years after the date of diagnosis.

These data, along with our previous findings showing that *Sema3B* levels are lower in the synovium of patients with early RA compared to patients with undifferentiated arthritis (8), which is considered an early phase of RA (38), confirm that expression of *Sema3B* is down-regulated during the progression of the disease. The pathogenic mechanisms observed in very early RA might be responsible for this reduction. In fact, IL-1 and TNF levels are elevated in the synovial fluid of patients with early RA (37), and the expression levels of *IL1B* and *TNF* negatively correlate with *SEMA3B* expression in the synovium of patients with early RA. In addition, both IL-1 and TNF down-regulate *Sema3B* expression in RA FLS (8). Nevertheless, we cannot rule out the possibility that ACPAs are involved in *Sema3B* expression, as serum *Sema3B* levels are increased in ACPA-positive RA patients and several studies have shown that anticitrullinated antibodies induce the expression of inflammatory mediators (38–40).

Taken together, our data from the K/BxN mouse model and human patients suggest that administration of *Sema3B* may be a new therapeutic approach for RA. Multiple studies have shown

that early treatment can prevent RA progression (41–43). Since Sema3B levels are low during the first year of the disease, early administration of Sema3B could prevent or decelerate the progression of joint damage and therefore preclude irreversible disability. Further studies are needed to analyze the therapeutic effect of Sema3B administration.

ACKNOWLEDGMENT

We thank Single Cell Discoveries for their help with the project design, single-cell sequencing services, and data analysis.

AUTHOR CONTRIBUTIONS

All authors were involved in drafting the article or revising it critically for important intellectual content, and all authors approved the final version to be published. Dr. García had full access to all of the data in the study and takes responsibility for the integrity of the data and the accuracy of the data analysis.

Study conception and design. Veale, Fearon, Conde, Pego-Reigosa, González-Fernández, Reedquist, Radstake, van der Helm-Van Mil, García.

Acquisition of data. Igea, Carvalheiro, Malvar-Fernández, Martínez-Ramos, Rafael-Vidal, Niemantsverdriet, Varadé, Fernández-Carrera, McGarry, Rodríguez-Trillo, García.

Analysis and interpretation of data. Igea, Carvalheiro, Malvar-Fernández, Martínez-Ramos, Rafael-Vidal, Niemantsverdriet, Jimenez, Reedquist, Radstake, van der Helm-Van Mil, García.

REFERENCES

- McInnes IB, Schett G. Pathogenetic insights from the treatment of rheumatoid arthritis. *Lancet* 2017;389:2328–37.
- Smolen JS, Aletaha D, Barton A, Burmester GR, Emery P, Firestein GS, et al. Rheumatoid arthritis. *Nat Rev Dis Prim* 2018;4:1–23.
- Aletaha D, Smolen JS. Diagnosis and management of rheumatoid arthritis: a review. *JAMA* 2018;320:1360–72.
- Sparks JA. Rheumatoid arthritis. *Ann Intern Med* 2019;170:ITC1–15.
- Garcia S. Role of semaphorins in immunopathologies and rheumatic diseases. *Int J Mol Sci* 2019;20:374.
- Gaur P, Bielenberg DR, Samuel S, Bose D, Zhou Y, Gray MJ, et al. Role of class 3 semaphorins and their receptors in tumor growth and angiogenesis. *Clin Cancer Res* 2009;15:6763–70.
- Worzfeld T, Offermanns S. Semaphorins and plexins as therapeutic targets. *Nat Rev Drug Discov* 2014;13:603–21.
- Tang MW, Malvar Fernández B, Newsom SP, va Buul JD, Radstake TR, Baeten DL, et al. Class 3 semaphorins modulate the invasive capacity of rheumatoid arthritis fibroblast-like synoviocytes. *Rheumatology (Oxford)* 2018;57:909–20.
- Ng CT, Biniiecka M, Kennedy A, McCormick J, FitzGerald O, Bresnihan B, et al. Synovial tissue hypoxia and inflammation in vivo. *Ann Rheum Dis* 2010;69:1389–95.
- Van Steenberg HW, Mangnus L, Reijniere M, Huizinga TW, van der Helm-van Mil AH. Clinical factors, anticitrullinated peptide antibodies and MRI-detected subclinical inflammation in relation to progression from clinically suspect arthralgia to arthritis. *Ann Rheum Dis* 2016;75:1824–30.
- Aletaha D, Neogi T, Silman AJ, Funovits J, Felson DT, Bingham CO III, et al. 2010 rheumatoid arthritis classification criteria: an American College of Rheumatology/European League Against Rheumatism collaborative initiative. *Arthritis Rheum* 2010;62:2569–81.
- Aletaha D, Neogi T, Silman AJ, Funovits J, Felson DT, Bingham CO III, et al. 2010 Rheumatoid arthritis classification criteria: an American College of Rheumatology/European League Against Rheumatism collaborative initiative. *Ann Rheum Dis* 2010;69:1580–88.
- Simmini S, Bialecka M, Huch M, Kester L, Van De Wetering M, Sato T, et al. Transformation of intestinal stem cells into gastric stem cells on loss of transcription factor Cdx2. *Nat Commun* 2014;5:1–10.
- Hashimshony T, Wagner F, Sher N, Yanai I. CEL-Seq: Single-Cell RNA-Seq by multiplexed linear amplification. *Cell Rep* 2012;2:666–73.
- Li H, Durbin R. Fast and accurate long-read alignment with Burrows-Wheeler transform. *Bioinformatics* 2010;26:589–95.
- Love MI, Huber W, Anders S. Moderated estimation of fold change and dispersion for RNA-seq data with DESeq2. *Genome Biol* 2014;15:1–21.
- Oliveros J. Venny: an interactive tool for comparing lists with Venn's diagrams. 2015. URL: <http://BioinfoGpCnbCsicEs/Tools/Venny/IndexHtml> 2015:2015.
- McInnes IB, Buckley CD, Isaacs JD. Cytokines in rheumatoid arthritis: shaping the immunological landscape. *Nat Rev Rheumatol* 2015;12:63–8.
- Sharma A, Verhaagen J, Harvey AR. Receptor complexes for each of the class 3 semaphorins. *Front Cell Neurosci* 2012;6:1–13.
- Miyabe Y, Lian J, Miyabe C, Luster AD. Chemokines in rheumatic diseases: pathogenic role and therapeutic implications. *Nat Rev Rheumatol* 2019;15:731–46.
- Lerner A, Neidhöfer S, Reuter S, Matthias T. MMP3 is a reliable marker for disease activity, radiological monitoring, disease outcome predictability, and therapeutic response in rheumatoid arthritis. *Best Pract Res Clin Rheumatol* 2018;32:550–62.
- Solomon S, Rajasekaran N, Jeisy-Walder E, Snapper SB, Ilges H. A crucial role for macrophages in the pathology of K/B × N serum-induced arthritis. *Eur J Immunol* 2005;35:3064–73.
- Wipke BT, Allen PM. Essential role of neutrophils in the initiation and progression of a murine model of rheumatoid arthritis. *J Immunol* 2001;167:1601–8.
- Monach PA, Nigrovic PA, Chen M, Hock H, Lee DM, Benoist C, et al. Neutrophils in a mouse model of autoantibody-mediated arthritis: critical producers of Fc receptor γ , the receptor for C5a, and lymphocyte function-associated antigen 1. *Arthritis Rheum* 2010;62:753–64.
- Müller-Ladner U, Kriegsmann J, Franklin BN, Matsumoto S, Geiler T, Gay RE, et al. Synovial fibroblasts of patients with rheumatoid arthritis attach to and invade normal human cartilage when engrafted into SCID mice. *Am J Pathol* 1996;149:1607–15.
- Lefèvre S, Knedla A, Tennie C, Kampmann A, Wunrau C, Dinsler R, et al. Synovial fibroblasts spread rheumatoid arthritis to unaffected joints. *Nat Med* 2009;15:1414–20.
- Xing Q, Feng J, Zhang X. Semaphorin3B promotes proliferation and osteogenic differentiation of bone marrow mesenchymal stem cells in a high-glucose microenvironment. *Stem Cells Int* 2021;2021:13–5.
- Sang C, Zhang Y, Chen F, Huang P, Qi J, Wang P, et al. Tumor necrosis factor α suppresses osteogenic differentiation of MSCs by inhibiting semaphorin 3B via Wnt/ β -catenin signaling in estrogen-deficiency induced osteoporosis. *Bone* 2016;84:78–87.
- Sabag AD, Smolkin T, Mumblat Y, Ueffing M, Kessler O, Gloeckner CJ, et al. The role of the plexin-A2 receptor in Sema3A and Sema3B signal transduction. *J Cell Sci* 2014;127:5240–52.
- Varshavsky A, Kessler O, Abramovitch S, Kigel B, Zaffryar S, Akiri G, et al. Semaphorin-3B is an angiogenesis inhibitor that is inactivated by furin-like pro-protein convertases. *Cancer Res* 2008;68:6922–31.
- Catalano A. The neuroimmune semaphorin-3A reduces inflammation and progression of experimental autoimmune arthritis. *J Immunol* 2010;185:6373–83.
- Teng Y, Yin Z, Li J, Li K, Li X, Zhang Y. Adenovirus-mediated delivery of Sema3A alleviates rheumatoid arthritis in a serum-transfer induced mouse model. *Oncotarget* 2017;8:66270–80.

33. Schett G, Tohidast-Akrad M, Smolen JS, Schmid BJ, Steiner CW, Bitzan P, et al. Activation, differential localization, and regulation of the stress-activated protein kinases, extracellular signal-regulated kinase, c-JUN N-terminal kinase, and p38 mitogen-activated protein kinase, in synovial tissue and cells in rheumatoid arthritis. *Arthritis Rheum* 2000;43:2501–12.
34. De Launay D, van de Sande MG, de Hair MJ, Grabiec AM, van de Sande GP, Lehmann KA, et al. Selective involvement of ERK and JNK mitogen-activated protein kinases in early rheumatoid arthritis (1987 ACR criteria compared to 2010 ACR/EULAR criteria): a prospective study aimed at identification of diagnostic and prognostic biomarkers as well as therapeutic targets. *Ann Rheum Dis* 2012;71:415–23.
35. Cush JJ, Splawski JB, Thomas R, McFarlin JE, Schulze-Koops H, Davis LS, et al. Elevated interleukin-10 levels in patients with rheumatoid arthritis. *Arthritis Rheum* 1995;38:96–104.
36. Bucht A, Larsson P, Weisbrot L, Thorne C, Pisa P, Smedegård G, et al. Expression of interferon-gamma (IFN- γ), IL-10, IL-12 and transforming growth factor-beta (TGF- β) mRNA in synovial fluid cells from patients in the early and late phases of rheumatoid arthritis (RA). *Clin Exp Immunol* 1996;103:357–67.
37. Raza K, Falciani F, Curnow SJ, Ross EJ, Lee CY, Akbar AN, et al. Early rheumatoid arthritis is characterized by a distinct and transient synovial fluid cytokine profile of T cell and stromal cell origin. *Arthritis Res Ther* 2005;7:R784–95.
38. Lu MC, Lai NS, Yu HC, Huang HB, Hsieh SC, Yu CL. Anti-citrullinated protein antibodies bind surface-expressed citrullinated Grp78 on monocyte/macrophages and stimulate tumor necrosis factor α production. *Arthritis Rheum* 2010;62:1213–23.
39. Dong X, Zheng Z, Lin P, Fu X, Li F, Jiang J, et al. ACPAs promote IL-1 β production in rheumatoid arthritis by activating the NLRP3 inflammasome. *Cell Mol Immunol* 2020;17:261–71.
40. Clavel C, Nogueira L, Laurent L, Iobagiu C, Vincent C, Sebbag M, et al. Induction of macrophage secretion of tumor necrosis factor α through Fc γ receptor IIa engagement by rheumatoid arthritis-specific autoantibodies to citrullinated proteins complexed with fibrinogen. *Arthritis Rheum* 2008;58:678–88.
41. Van Nies JA, Tsonaka R, Gaujoux-Viala C, Fautrel B, Van Der Helm-Van Mil AH. Evaluating relationships between symptom duration and persistence of rheumatoid arthritis: does a window of opportunity exist? Results on the Leiden Early Arthritis Clinic and ESPOIR cohorts. *Ann Rheum Dis* 2015;74:806–12.
42. Van Der Linden MP, Le Cessie S, Raza K, Van Der Woude D, Knevel R, Huizinga TW, et al. Long-term impact of delay in assessment of patients with early arthritis. *Arthritis Rheum* 2010;62:3537–46.
43. Van Der Woude D, Young A, Jayakumar K, Mertens BJ, Toes RE, van der Heijde, et al. Prevalence of and predictive factors for sustained disease-modifying antirheumatic drug-free remission in rheumatoid arthritis: results from two large early arthritis cohorts. *Arthritis Rheum* 2009;60:2262–71.